System Identification and Robust Controller Design for the Autopilot of an Unmanned Helicopter

Ahmad Safaee
Electrical Engineering Faculty
Shahid Rajaee University
Tehran, Iran
safaeeahmad@gmail.com

Hamid D. Taghirad
Electrical Engineering Faculty
K.N. Toosi University of technology
Tehran, Iran
taghirad@kntu.ac.ir

***Abstract*—One of the most complex issues which are proposed in designing a controller for autopilots is robustness. This requirement is due to the dynamic model changes and also, the resistance to environmental disturbances. A main factor that changes the dynamic model of the helicopter autopilot is any change in body mass center, such as any additional load. Furthermore, wind is one of the main causes of environmental disturbances. In this paper model identification of four systems in helicopter by using real data is presented. For all systems robust H2/H∞ and mixed sensitivity controller are designed. The simulation results show the robustness of designed controllers in the existence of uncertainty. The designed controller was implemented on the real case study. Results demonstrate the robustness of the system.**

Keywords—autopilot; helicopter; robust controller; H2/H∞; mixed sensitivity

I. INTRODUCTION

In recent years, research and development of unmanned vehicles have gained much attention both in the academic and military communities. They are developed to be capable of working automatically without interference of a human pilot. The main problem in the operation of these vehicles is the various situations that they need to deal with. For instance, much complicated and uncertain environments, such as unexpected obstacles, enemies attacking and device failures are serious challenges. Besides, they are required to communicate with technical personnel in the ground station. a wide range of factors should be taken into consideration. Software systems for unmanned vehicles are required to perform multi-level tasks, such as from hardware driving to device operation management.

Among various unmanned aerial vehicles (UAVs), small-scale unmanned helicopters are an ideal platform for research purposes. Besides having the characteristics of full-scale rotorcraft, it owns some unique and attractive features such as low cost, easy operation, and extreme quickness. During the last two decades, many research groups have chosen such platforms for their research purposes [1,2,3].

In the robust multivariable control theory, the plant uncertainty is the main focus in order to design a robust controller with guaranteed performance. If there are uncertainties in the system model, some quantity combining the H2 norm and the H∞ norm can be a desirable measure of a system's robust performance [4]. Thus the mixed H2/H∞ performance criterion provides an interesting measure for evaluating controllers. The theoretic motivation for the mixed H2/H∞ control problem has been extensively explained in [5, 6, 7, 8].

The remaining part of the paper is organized as follows. Section II defines the system hardware and software. The nominal model and uncertainty profile is proposed in section III. In section IV, the uncertainty profile limits will be determined. The controller design with mixed sensitivity and H2/H∞ method is presented in section V and VI. Finally last section concludes the paper.

II. SYSTEM HARDWARE AND SOFTWARE

A. Hardware

In this paper, a brand Trex-600 electric helicopters of Align Company is used. Selection of this type of helicopter is in order to eliminate the produced noise of gasoline engines vibration on the operation of sensors and also, autopilot system. Fig. 1 illustrates the TREX-600 helicopter equipped with an autopilot system.

Flight computer, is an industrial computer, PC104 which has the processing speed of 800 MHz and has 4 serial ports, 256Mb RAM and the HDD 1Gb. Servo control circuit, transceiver RF, sensor, GPS / INS are connected directly to the computer's serial port.

Fig. 1. TREX-600 helicopter equipped with an autopilot system.

On this computer, the software of autopilot and communication modules with GPS / INS, servo control circuit and communication with the ground station are implemented via RF. Also, servo control circuit and communication with the ground station are implemented via the RF circuit. In order to obtain the position angle, heading, linear velocity and position in a three-axis, sensor GPS / INS MTI-G model manufactured by XSENS is used. Circuit interface includes an FMS and Servo controller. FMS task is changing flights' modes between the auto pilot and manual flight from long distance, removing some noises inside the system and also, is necessary to rescue helicopter fall because of autopilot failing in testing period. Servo controller is a circuit that includes an ATMEGA128 microcontroller and a MAX232 and produce PWM pulse that is required for the servo. To exchange and collect information a modem module, RF Xbee with a range of about 1 km is used. System ground control station includes a laptop, a Joystick and a RF that is able to communicate online with helicopter and in addition to receiving flight information, increase or decrease profile flying missions or update the waypoint. The ground control station is shown in Fig. 2, and Fig. 3 illustrates General chart of flight system hardware.

Fig. 2. Ground control station.

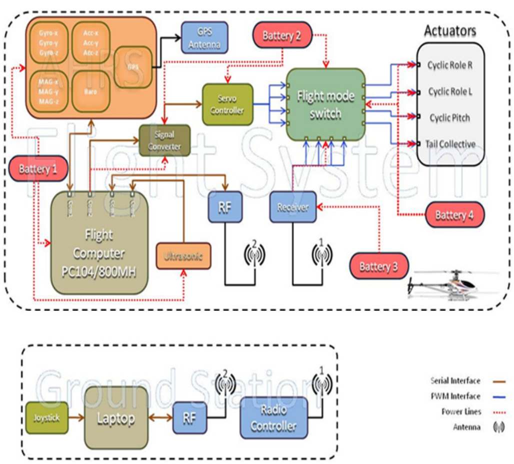

Fig. 3. General chart of flight system hardware.

B. Software

Software of autopilot system is implemented with the approach of object-oriented and in the form of high-level class structures which has two main parts, ground station software and autopilot software. Ground Station software includes necessary features to display and control the status of the helicopter. Autopilot software includes implemented controller. Autopilot software that runs on the flight computer is set of classes that are directly or indirectly related to each other, and is implemented in C#.net programming environment under the DOS operating system. The ground station software is implemented in C programming environment under the Windows XP system and has a graphical environment for helicopter information illustration such as information about position angles, navigation and autopilot parameters change.

For flight information storage, flight data are stored in flight computer in a real time manner and after flight testing is callback from computer and used. In this method, the sampling frequency is set to 100 (Hz) increased. In this mode joystick commands that are issued by the pilot, is applied to the operator directly, the helicopter flight is completely manual in this mode. So, the different types of flight conditions without angular limits for the helicopter are done to obtain the open-loop system data. This enables the storage of sensor output and also, the issued commands to the operator. The obtained data is used in this paper for different purposes.

Fig. 4 is shown the software modules of the system.

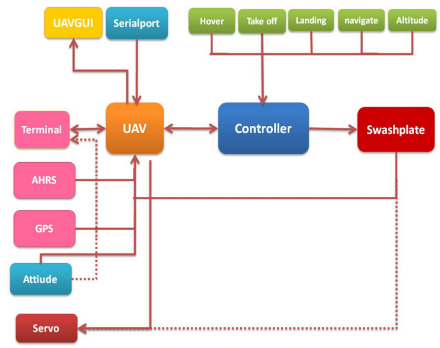

Fig. 4. Software modules of the system.

III. NOMINAL SYSTEM IDENTIFICATION

In this section, with the real input-output data of helicopter, system identification is performed on 4 data categories. These 4 categories are shown in Table. 1.

TABLE I. SYSTEM CATEGORIES FOR IDENTIFICATION

Input	***Output***	***Transfer Function***
Tail collective	Yaw	G_1
Roll Cyclic	Roll	G_2
Pitch Cyclic	Pitch	G_3
Collective	Altitude	G_4

Among input-output system identification for each pair, a nominal system is achieved and an uncertainty profile is obtained. Nominal model is based on having the least uncertainty profile particularly in low frequencies. Identifications are based on Box-Jenkins method. In the next parts with the information of nominal model and multiplicative uncertainty profile, robust controller is designed for each system.

A. Tail collective-yaw system

In the first system the tail collective is input and yaw is output. The identified systems' bode diagrams are plotted in Fig. 5. Nominal system is achieved as equation (1).

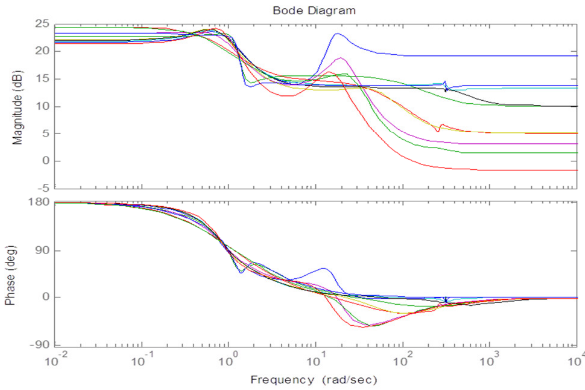

Fig. 5. Bode diagram of identified system G_1.

B. *Roll Cyclic-roll system*

In the second system with roll cyclic-roll as input-output, the identified systems' bode diagrams are plotted in Fig. 6. Nominal system is achieved as equation (2).

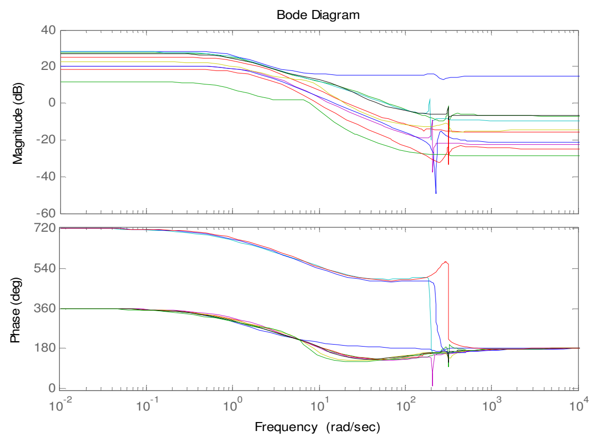

Fig. 6. Bode diagram of identified system G_2.

C. *Pitch cyclic-pitch system*

Third categories of input-outputs are pitch cyclic-pitch. The identified systems' bode diagrams are plotted in Fig. 7 and nominal model in shown in equation (3).

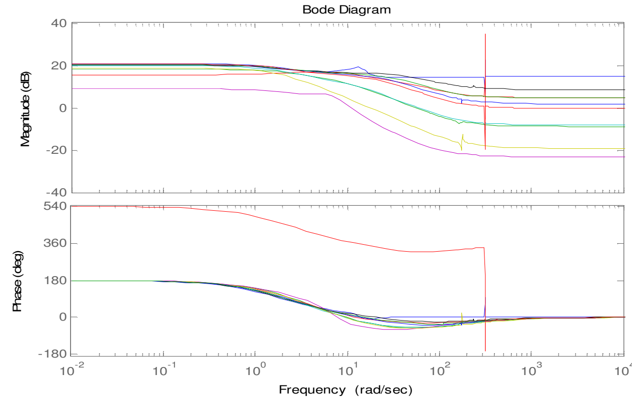

Fig. 7. Bode diagram of identified system G_3.

D. *Collective-altitude system*

The last input-output category is collective-altitude. The identified systems' bode diagrams of this case are plotted in Fig. 8 and nominal model in shown in equation (4).

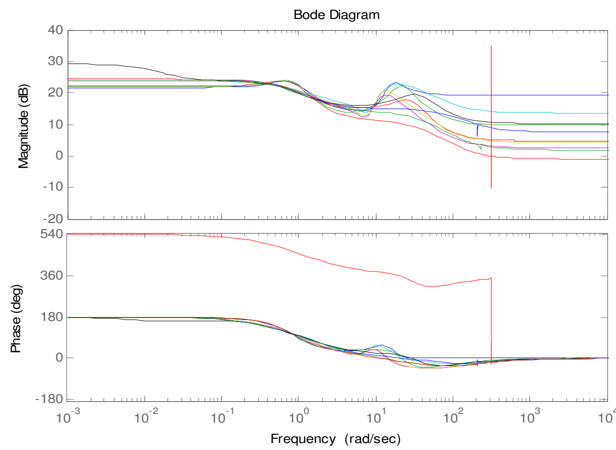

Fig. 8. Bode diagram of identified system G_4.

$$G_1(s) = \frac{1.773s^5 + 210.8s^4 + 1.84 \times 10^5 s^3 + 1.68 \times 10^7 s^2 + 3.69 \times 10^8 s - 7.97 \times 10^8}{s^5 + 50.24s^4 + 1.002 \times 10^5 s^3 + 2.67 \times 10^6 s^2 + 7.75 \times 10^7 s + 4.99 \times 10^7} \tag{1}$$

$$G_2(s) = \frac{-0.16s^4 - 21.85s^3 - 4503s^2 - 5.46 \times 10^5 s + 5.68 \times 10^6}{s^4 + 24.65s^3 + 2.82 \times 10^4 s^2 + 2.75 \times 10^5 s + 3.14 \times 10^5} \tag{2}$$

$$G_3(s) = \frac{0.3937s^4 + 53.93s^3 + 3.82 \times 10^4 s^2 + 5.25 \times 10^6 s - 2.17 \times 10^7}{s^4 + 14.68s^3 + 9.76 \times 10^4 s^2 + 1.39 \times 10^6 s + 2.24 \times 10^6} \tag{3}$$

$$G_4(s) = \frac{1.73s^5 + 181.6s^4 + 1.75 \times 10^5 s^3 + 1.79 \times 10^7 s^2 + 4.1 \times 10^8 s - 9.03 \times 10^8}{s^5 + 29.35s^4 + 9.95 \times 10^4 s^3 + 2.89 \times 10^6 s^2 + 8.57 \times 10^7 s + 5.52 \times 10^7} \tag{4}$$

IV. UNCERTAINTY PROFILE LIMIT

In each system the uncertainty profile W is achieved to have equation (5) correct.

$$\left|\frac{p}{p_0} - 1\right| \leq W \tag{5}$$

Where p is the set of plants, and p_0 is nominal plant. The bode diagram of obtained profiles are and plotted in Fig. 9-12.

One should choose the uncertainty profile limit such that covers the worst case of uncertainty. In each figure it is plotted in --blue. These limits are shown in equation 6-9.

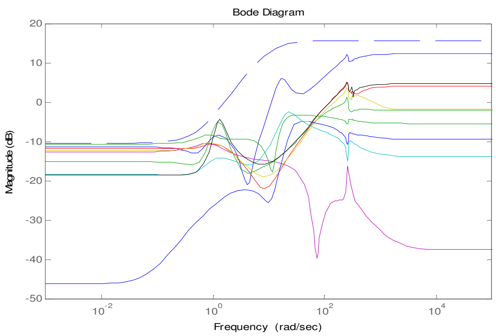

Fig. 9. Bode diagram of uncertainty profile for G_1

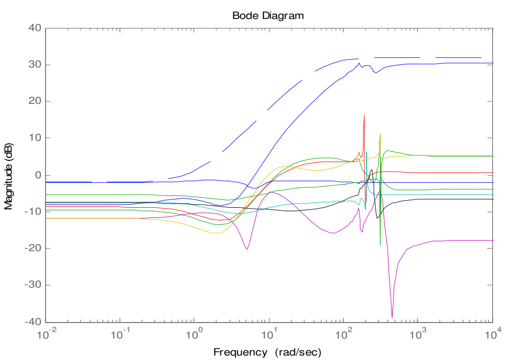

Fig. 10. Bode diagram of uncertainty profile for G_2.

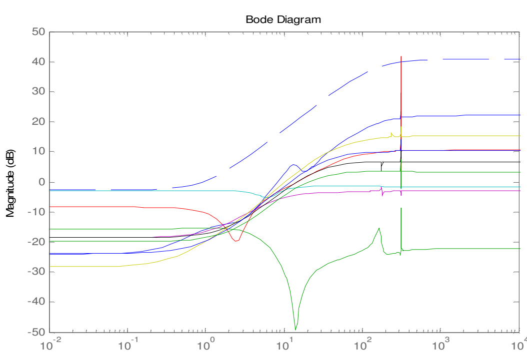

Fig. 11. Bode diagram of uncertainty profile for G_3.

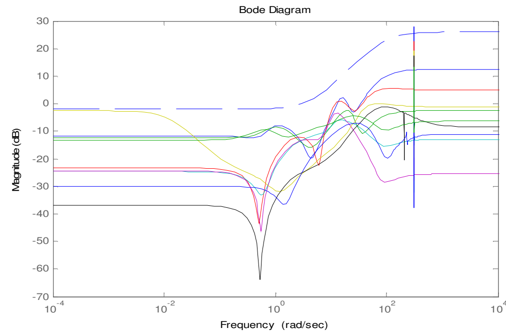

Fig. 12. Bode diagram of uncertainty profile for G_4.

$$W_{T_1}(s) = 6\left(\frac{s+0.5}{s+10}\right) \tag{6}$$

$$W_{T_2}(s) = 40\left(\frac{s+1}{s+50}\right) \tag{7}$$

$$W_{T_3}(s) = 110\left(\frac{s+1}{s+150}\right) \tag{8}$$

$$W_{T_4}(s) = 20\left(\frac{s+4}{s+100}\right) \tag{9}$$

As illustrated in all figures the considered W_{T} cover all uncertainties of the system.

V. CONTROLLER DESIGN WITH MIXED SENSITIVITY

In this part, a robust controller by mixed sensitivity consideration is designed for each system.

Controller design is based of having overshoot less than 15% and settling time less than 4s. So the desired system is $T_{id} = \frac{5.06}{s^2+2.3s+5.06}$ and sensitivity function becomes $S_{id} = 1 - T_{id} = \frac{s(s+2.3)}{s^2+2.3s+5.06}$, finally W_s for all 4 systems is defined in equation 10-13.

$$W_{s1} = 0.3\frac{s^2+2.3s+5.06}{(s+0.001)(s+2.3)(0.001s+1)} \tag{10}$$

$$W_{s2} = 0.2\frac{s^2+2.3s+5.06}{(s+0.001)(s+2.3)(0.001s+1)} \tag{11}$$

$$W_{s3} = 0.2\frac{s^2+2.3s+5.06}{(s+0.001)(s+2.3)(0.001s+1)} \tag{12}$$

$$W_{s4} = 0.2\frac{s^2+2.3s+5.06}{(s+0.001)(s+2.3)(0.001s+1)} \tag{13}$$

Suppose W_u=1. In mixed sensitivity problems, the objective is to set uncertainty transfer functions such that:

$$\gamma_{opt} = min\left\|\begin{matrix} WT \\ W_s S \\ W_u U \end{matrix}\right\|_\infty \leq 1 \tag{14}$$

Design parameters for all systems are plotted in Fig. 13-16. In the figures γ_{opt} is displayed as sigma. It is clear that in all cases, equation (14) is justified. Values of γ_{opt} for the four systems are: $\gamma_{opt-1} = 0.95$, $\gamma_{opt-2} = 0.92$, $\gamma_{opt-3} = 0.92$, $\gamma_{opt-4} = 0.94$,

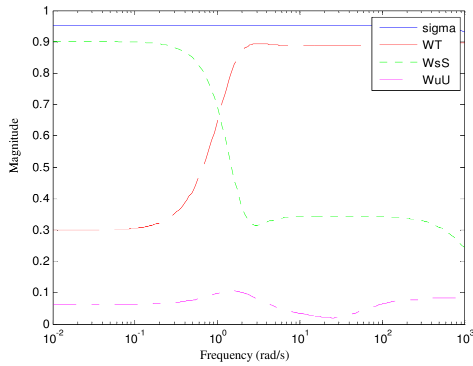

Fig. 13. Design parameters for G_1 in mixed sensitivity case.

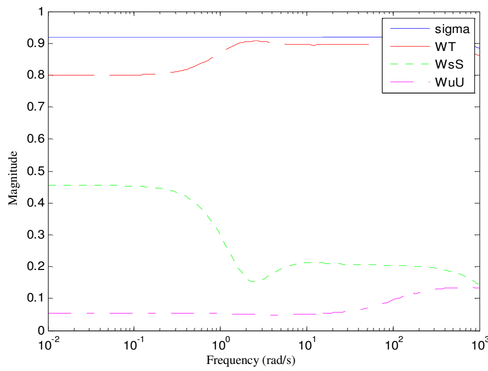

Fig. 14. Design parameters for G_2 in mixed sensitivity case.

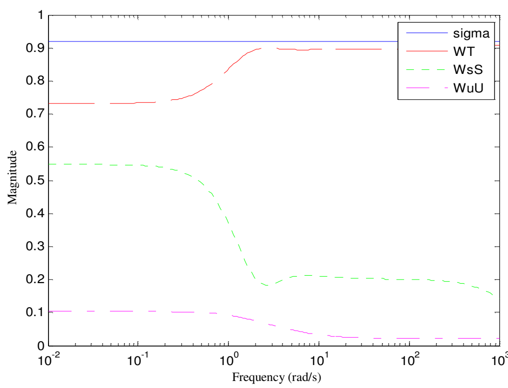

Fig. 15. Design parameters for G_3 in mixed sensitivity case.

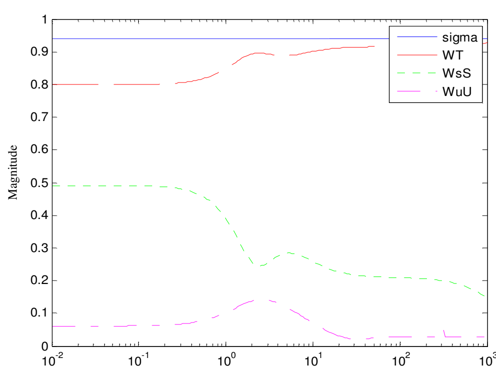

Fig. 16. Design parameters for G_4 in mixed sensitivity case.

All systems are robustly stable, and sigma plot is flat. Second and infinity norm of control signal for nominal systems are shown in Table. II.

TABLE II. SECOND AND INFINITY NORM OF CONTROL SIGNAL

Nominal System	*Second Norm*	*Infinity Norm*
G_1	4.26	0.1
G_2	5.72	0.13
G_3	2.96	0.1
G_4	2.99	0.14

VI. CONTROLLER DESIGN WITH H2/H∞ METHOD

Consider all nominal systems G_1, G_2, G_3, G_4 and W_T, W_S and W_U which were derived before. Based on [9], the robust controller is designed to justify equation 15.

$$\min_{\gamma_{opt}} \left\| \begin{matrix} W_S S \\ W_T T \end{matrix} \right\|_\infty < 1 \quad , \|W_u u\|_\infty < 1 \qquad (15)$$

Design parameters for all systems are plotted in Fig. 17-20. It is clear that in all cases, equation (15) is justified.

All systems are robustly stable. The γ related to second and infinity norm are shown in Table. III.

TABLE III. THE γ RELATED TO SECOND AND INFINITY NORM.

Nominal System	$\gamma_{H\infty}$	γ_{H2}
G_1	1.01	1
G_2	0.92	1
G_3	0.91	1
G_4	0.95	1

The values of γ is suitable for engineering work.

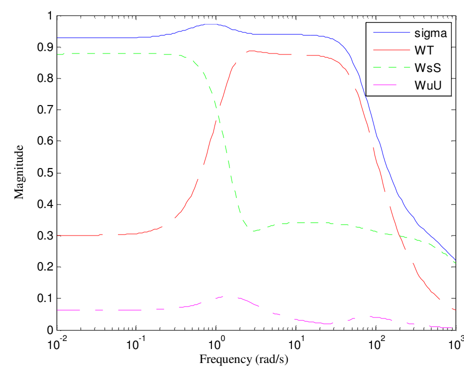

Fig. 17. Design parameters for G_1 in H2/H∞ case.

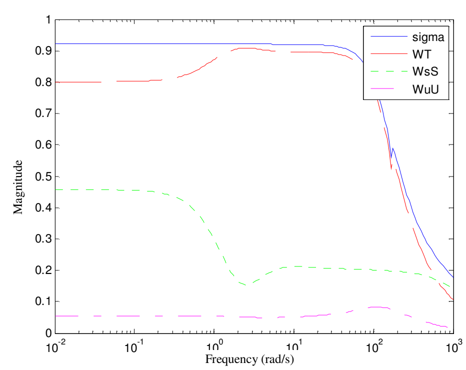

Fig. 18. Design parameters for G_2 in H2/H∞ case.

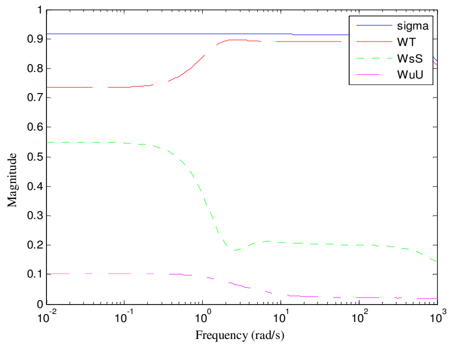

Fig. 19. Design parameters for G_3 in H2/H∞ case.

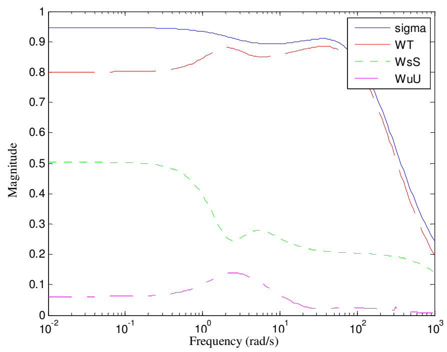

Fig. 20. Design parameters for G_4 in H2/H∞ case.

Orders of designed controllers are generally 11 to 14, with reduce function they become 4 or 5. The controllers are checked with μ synthesis. With taking them to z space, we realize them.

The controllers are implemented in real autopilot and helicopter is flown semi-automatically. The results of implementation are shown in Fig. 21.

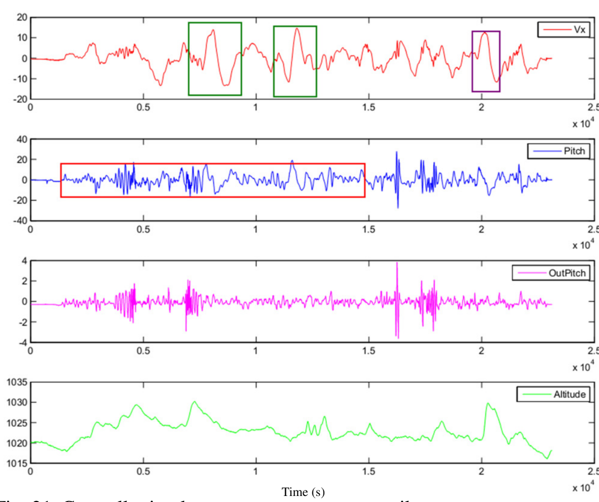

Fig. 21. Controller implementation on a real autopilot.

When a controller is designed, first of all one should test it on ground and check the control response. Previously, in different flight tests, we tune the proportional gains of PID controllers, that for roll and pitch loop they were about 0.07. At low frequencies before flight, we switch between previous PID controllers and robust controllers; the behavior was similar that we take courage to fly helicopter.

In Fig. 21. that is for flight testing, autopilot is on stick mode, means that desired values of yaw, pitch and roll loops are taken from simulator or joy stick and system operate in closed loop manner. In different axis, operator commands the helicopter and play with it to examine the controller robustness and does forward and backward flight with it. Note that in this test altitude loop is not closed and for more immunity the collective command is manually. In this figure the first plot is speed. The first and second green rectangular are related to forward speed and the speed is about $15\ m/s$ or equally $54\ km/h$. After that backward flight is done with lower speed about $35\ km/h$. In violet rectangular both forward flight and altitude changes are done. In the second plot that show the pitch angle, the red rectangular shows that pitch angle is limited between $\pm 20°$ that is pitch loop saturation.

CONCLUSION

In this paper, the identification of 4 systems in unmanned helicopter is done. For each system the nominal model and uncertainty profile limit is achieved. The robust controllers are designed for all systems and in two manners H2/H∞ and mixed sensitivity method. The simulation results illustrate the proficiency of designed controllers to track the desired values. The controllers are implemented in real autopilot. Results of implementation justify the capability of robust controllers.

REFERENCES

[1] Kim HJ, Shim DH, Sastry S. Flying robots: modeling, control and decision making. In: Proceedings of the 2002 IEEE international conference on robotics and automation, Washington, DC; 2002. p. 66–71.

[2] Roberts JM, Corke P, Buskey G. Low-cost flight control system for a small autonomous helicopter. In: Proceedings of the 2002 Australasia conference on robotics and automation, Auckland, New Zealand; 2002. p. 546–51.

[3] Shim DH, Kim HJ, Sastry S. Decentralized nonlinear model predictive control of multiple flying robots. In: Proceedings of the 42nd IEEE conference on decision and control, Maui, Hawaii; 2003. p. 3621–6.

[4] K. Zhou, K. Glover and B. Bodenheimer and J. Doyle, "Mixed H2 and H∞ Performance Objectives I: Robust Analysis", in IEEE Transactions on Automatic Control, vol. 39, no. 8, 1994, pp. 1564-1574.

[5] D.S. Bernstein and W.M. Haddad, "LQG Control with an H∞ Performance Bound: A Riccati Equation Approach", in IEEE Transactions on Automatic Control, vol. 34, no. 3, 1989, pp. 293-305.

[6] J. Doyle, K. Zhou, K. Glover and B. Bodenheimer, "Mixed H2 and H∞ Performance Objectives II: Optimal Control", in IEEE Transactions on Automatic Control, vol. 39, no. 8, 1994, pp. 1575-1586

[7] P.K. Khargonekar and M.A. Rotea, "Mixed H2/H∞ Control: A Convex Optimization Approach", in IEEE Transactions on Automatic Control, vol. 36, no. 7, 1991, pp. 824-837.

[8] C. Scherer, "Mutiobjective H2/H∞ Control", in IEEE Transactions on Automatic Control, vol. 40, no. 6, 1995, pp. 1054-1062

[9] J. Doyle, K. Glover, P. P. Khargonekar, State Space Solutions to Standard H2 and H∞ Control Problems, IEEE Transaction on Automation Control, August 1989.